THE JOURNAL OF PHYSICAL CHEMISTRY LETTERS
A JOURNAL OF THE AMERICAN CHEMICAL SOCIETY

pubs.acs.org/JPCL

Letter

Time-Resolved X-ray Photoelectron Spectroscopy: Ultrafast Dynamics in CS_2 Probed at the S 2p Edge

Ian Gabalski, Felix Allum, Issaka Seidu, Mathew Britton, Günter Brenner, Hubertus Bromberger, Mark Brouard, Philip H. Bucksbaum, Michael Burt, James P. Cryan, Taran Driver, Nagitha Ekanayake, Benjamin Erk, Diksha Garg, Eva Gougoula, David Heathcote, Paul Hockett, David M. P. Holland, Andrew J. Howard, Sonu Kumar, Jason W. L. Lee, Siqi Li, Joseph McManus, Jochen Mikosch, Dennis Milesevic, Russell S. Minns, Simon Neville, Atia-Tul-Noor, Christina C. Papadopoulou, Christopher Passow, Weronika O. Razmus, Anja Röder, Arnaud Rouzée, Alcides Simao, James Unwin, Claire Vallance, Tiffany Walmsley, Jun Wang, Daniel Rolles, Albert Stolow, Michael S. Schuurman,* and Ruaridh Forbes*

Cite This: *J. Phys. Chem. Lett.* 2023, 14, 7126−7133

Read Online

ACCESS | Metrics & More | Article Recommendations | Supporting Information

ABSTRACT: Recent developments in X-ray free-electron lasers have enabled a novel site-selective probe of coupled nuclear and electronic dynamics in photoexcited molecules, time-resolved X-ray photoelectron spectroscopy (TRXPS). We present results from a joint experimental and theoretical TRXPS study of the well-characterized ultraviolet photodissociation of CS_2, a prototypical system for understanding non-adiabatic dynamics. These results demonstrate that the sulfur 2p binding energy is sensitive to changes in the nuclear structure following photoexcitation, which ultimately leads to dissociation into CS and S photoproducts. We are able to assign the main X-ray spectroscopic features to the CS and S products via comparison to a first-principles determination of the TRXPS based on *ab initio* multiple-spawning simulations. Our results demonstrate the use of TRXPS as a local probe of complex ultrafast photodissociation dynamics involving multimodal vibrational coupling, nonradiative transitions between electronic states, and multiple final product channels.

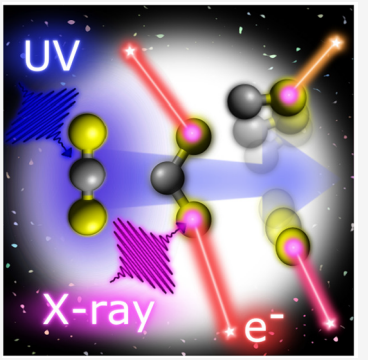

The ultrafast dynamics that occur in electronically excited states of molecules are often characterized by strong non-adiabatic coupling between electronic and vibrational degrees of freedom. Elucidation of such coupling remains an enduring challenge for experimental techniques. In the constellation of spectroscopic methods, time-resolved photoelectron spectroscopy (TRPES) has emerged as a particularly effective approach for studying ultrafast dynamics in isolated molecules.[1−5] The dependence of the electron binding energies, photoionization cross sections, and photoelectron angular distributions on the evolving nuclear-electronic character of a molecular wave packet permits time-resolved probing of ultrafast non-adiabatic dynamics with femtosecond ultraviolet (UV) or vacuum ultraviolet (VUV) pulses.[6−13] Furthermore, simulation of these spectroscopic observables via quantum dynamics techniques provides the ability to correlate experimental observables with the underlying electronic and nuclear dynamics, often leading to highly detailed descriptions of photochemical processes.[14−16]

The advent of soft X-ray free-electron lasers (FELs) has enabled the photoionization of highly localized core−shell electrons, permitting an atom-specific view of ultrafast electronic and nuclear dynamics within molecules.[17−20] Furthermore, given the large energy separation between the core ionization potentials of differing atoms, a novel, multidimensional view of molecular wave packets emerges from probing these dynamics from the perspectives of different atoms.[21] Here we present the results of a joint theoretical−experimental proof-of-concept study of the sensitivity of the time-resolved X-ray photoelectron spectroscopy (TRXPS) technique to the complex multichannel UV photodissociation of carbon disulfide (CS_2) probed via photoionization above the sulfur 2p edge.

Initial TRXPS studies of the atomic site-specific chemical shifts induced by non-adiabatic and photodissociation dynamics have shown promising results. The work of Wernet and co-workers identified distinct photodissociation products of $Fe(CO)_5$ from shifts in the Fe 3p binding energy.[17] Recent work by Braußе et al. and Allum et al. revealed variation in the

Received: May 25, 2023
Accepted: July 17, 2023
Published: August 3, 2023

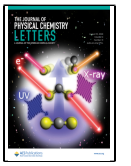

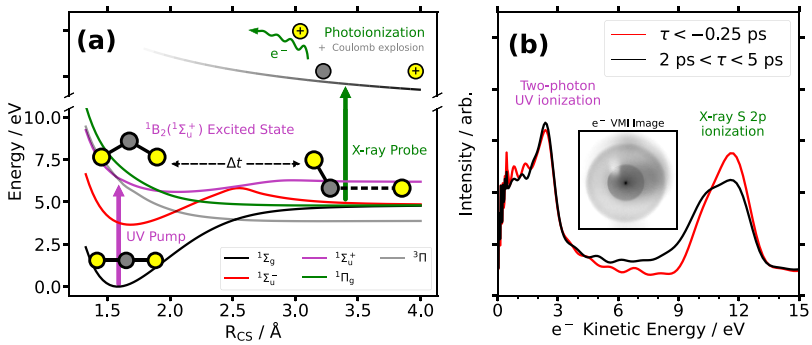

Figure 1. (a) Cartoon of the relevant potential energy surfaces of CS_2. The UV photoexcitation (purple arrow), time evolution of the molecular system, and X-ray photoionization (green arrow) processes are shown alongside cartoons of the approximate CS_2 geometry and charge state at each step. (b) Measured CS_2 photoelectron kinetic energy spectrum for pre-time zero ("$\tau < -0.25$ ps", red) and late time ("2 ps $< \tau <$ 5 ps", black). The peak at 2.23 eV is due to two-photon ionization of ground-state CS_2 by the UV pump alone. The inset shows an illustrative photoelectron VMI detector image that is subsequently Abel-inverted to obtain the spectra in the figure.

iodine core level (I 4d) binding energy due to photodissociation of iodoalkanes.[18,19] While the time-resolved photoelectron spectra in each of these prior experiments demonstrate the possibility of using core level binding energy shifts to detect chemical changes, they each suffer from either a lack of time resolution relative to the dynamics of interest[17,19] or a lack of sensitivity to multiple photoproducts.[18] Of particular relevance to the work presented here is a study by Gühr and co-workers, who investigated the ultrafast non-adiabatic relaxation of photoexcited 2-thiouracil by observing excited-state sulfur 2p chemical shifts.[20] Their observations of both coherent charge migration at the sulfur probe site and ultrafast relaxation back to the ground state constitute an important step in the use of TRXPS to track ultrafast dynamics in molecules.

The results reported here comprise a significant extension of the TRXPS technique to the complex multichannel UV photochemistry of CS_2, a benchmark system for studying ultrafast photodissociation. Upon photoexcitation at 200 nm, the optically bright $^1\Sigma_u^+$ state couples strongly to the $^1\Pi_g$ state (violet and green curves in Figure 1a), mediated by large-amplitude nuclear motion along the bending and asymmetric stretch vibrational coordinates. Dissociation is observed to both singlet S(^{1}D) and triplet S(^{3}P) photoproducts, the latter realized following intersystem crossing on subpicosecond time scales.[7,10,22,23] This dissociation also produces a CS fragment with a channel-dependent vibrational distribution.[23,24] The ultrafast excited-state dynamics have been investigated previously, most notably in a number of valence TRPES studies,[7,9−11,25−27] as well as more recently through coherent diffractive imaging with ultrafast electrons and X-rays.[28,29] The work presented here extends both the prior time-resolved CS_2 studies and the TRXPS studies of other molecules by demonstrating the sensitivity of inner-shell spectral observables to the complex multidimensional vibration and photodissociation of CS_2.

In Figure 1a, we depict the ultrafast dynamics on the excited-state potential energy curves, as well as the photoionization probe process. Gas-phase CS_2 was photoexcited with a femtosecond 201.5 nm pump pulse. The subsequent dynamics were probed via photoionization above the S 2p edge ($2p_{3/2}$ at 169.98 eV and $2p_{1/2}$ at 171.17 eV[30]) using 181.5 eV soft X-ray pulses at the free-electron laser in Hamburg (FLASH).[31] Photoelectrons and ion fragments were detected in a double-sided velocity map imaging (VMI) instrument.[32] In the work presented here, we focus on the energy-resolved TRXPS signals extracted from the photoelectron images as a function of the pump−probe delay. The ion data will be presented in a separate manuscript.[33] A more detailed account of the experimental apparatus and the data processing steps is given in Methods and the Supporting Information.

To interpret the experimental TRXPS in terms of the underlying non-adiabatic dynamics, we employ an *ab initio* multiple-spawning (AIMS) description of the dynamics within the singlet manifold of electronic states in conjunction with high-level quantum chemical computations of the core ionization cross sections.[34] The time-resolved AIMS simulations include only the singlet manifold of states and thus will not describe the intersystem crossing process or the triplet dissociation channel. The core ionization cross sections of the products of triplet sulfur dissociation, including both triplet atomic sulfur and the vibrationally excited CS fragment, are still computed for the purposes of the spectral assignment. Details of the AIMS simulations and computation of associated spectral observables are described in Methods, with further details in the Supporting Information. The experimental and simulated TRXPS signals are directly compared to assign features of the experimental TRXPS spectrum. These combined experimental and theoretical results demonstrate the general utility of TRXPS as a probe of complex photochemical dynamics.

Experimental TRXPS spectra of CS_2 integrated over two delay ranges within which the UV radiation precedes the X-ray (and vice versa) are shown in Figure 1b. To improve the spectral resolution of the experiment, we remove blurring due to FEL spectral jitter. This is accomplished by sorting FEL shots on the basis of their mean photon energy, computing the photoelectron spectrum for each mean photon energy bin, and then shifting and summing the individual spectra appropriately. Spectral correlation techniques such as spectral domain ghost imaging[35,36] could have provided improved spectral resolution, but we found our statistics insufficient for a full time-resolved treatment with these techniques. Full details of the data collection and analysis, including spectra both with and without this shifting procedure, are shown in the Supporting Information. The primary photoelectron signal from FEL-ionized ground-state CS_2 is located around 11.5 eV (~170 eV binding energy). Comparison between the pre-time-zero spectrum (red line, "$\tau < -0.25$ ps") and the late-time spectrum (black line, "2 ps $< \tau <$ 5 ps") shows significant changes in the region between 5 and 13 eV, consistent with a depletion of the signal from ground-state CS_2 and enhancements due to the

https://doi.org/10.1021/acs.jpclett.3c01447
J. Phys. Chem. Lett. 2023, 14, 7126−7133

emergence of photoproducts having higher binding energies. The relatively narrow peak centered at 2.23 eV arises from two-photon ionization of ground-state CS_2 by the UV pump pulse.

The experimental TRXPS spectrum, plotted as a difference signal following subtraction of the pre-time-zero spectrum, is shown in Figure 2a as a function of both photoelectron kinetic energy (eKE) and pump−probe delay. The data show the depletion of the ground-state CS_2 S 2p ionization signal at 11.5 eV and a range of enhancements between 5 and 10 eV photoelectron energies. The pre-time-zero and late-time spectra are shown for reference on the right in red and black, respectively. To aid in the assignment of these spectral features, we compare them to a simulated TRXPS extracted from AIMS simulations of photoexcited CS_2. The simulated TRXPS difference signal is shown in Figure 2b. The AIMS simulations were terminated after ∼1 ps, because the preponderance of the CS_2 population had dissociated by this time. Highlighted in Figure 2b are three spectral regions of interest: (i) an immediate broad depletion superimposed with a brief transient enhancement at a photoelectron energy of 11.5 eV, (ii) a broad spectrum of enhancements between 6 and 10 eV that evolves in the first several hundred femtoseconds (see also Figure 2c), and (iii) long-lived enhancements at 6.5 and 8.5 eV. Using the computed static spectra in Figure 3 as a guide, we assign the broad depletion at 11.5 eV to the prompt bleaching of the ground-state CS_2 signal, while the narrow enhancement originates from the initially populated $^1\Sigma_u^+$ state in the Franck−Condon region. The Franck−Condon region excited-state signal decays rapidly due to its large-amplitude, coupled stretch−bend dynamics, which induce a large range of chemical shifts down to a photoelectron energy of 6 eV. The large-amplitude bend is associated with a non-adiabatic mixing of Σ_u^+ with Π_g electronic character, due to the pseudo-Renner−Teller effect.[25] Dissociation to atomic sulfur occurs throughout this period, generating asymptotic photoelectron signals from S(^{1}D) and the CS fragment between 5 and 10 eV with long time delays.

The agreement between the simulated and experimental time-resolved spectra is encouraging. Both are broadly characterized by a depletion in the ground-state CS_2 signal and two distinct regions of signal enhancement at a higher binding energy (lower eKE). The primary discrepancy between the simulated and experimental TRXPS is that of the time scale. Figure 2c compares experimental and theoretical signals as a function of pump−probe delay gated over several distinct regions of

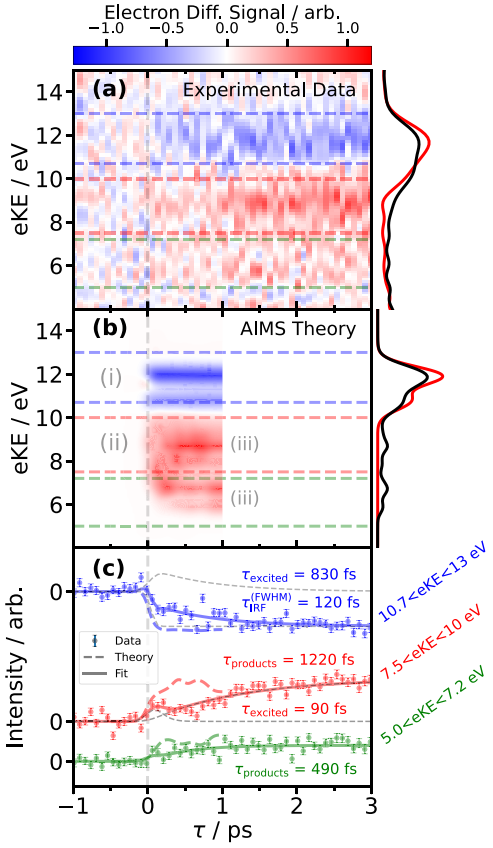

Figure 2. (a) Experimental TRXPS difference signal as a function of pump−probe delay τ and electron kinetic energy (eKE). Pre-time-zero (red, "$\tau < -0.25$ ps") and late-time (black, "2 ps $< \tau <$ 5 ps") spectra are shown beside the time-resolved difference signal. (b) Simulated TRXPS difference signal calculated using an ensemble of singlet AIMS trajectories. Three regions of interest (i−iii) described in the text are indicated. (c) Energy-integrated time-dependent intensities of the TRXPS data (dots with error bars) and theory (dashed colored lines), signal fits (solid colored lines), and the components of the signal fits (gray dashed lines). The instrument response function (IRF), excited-state, and photoproduct time constant parameter fits are indicated alongside each curve. The energy integration bounds are indicated with translucent colored dashed lines in panels a and b.

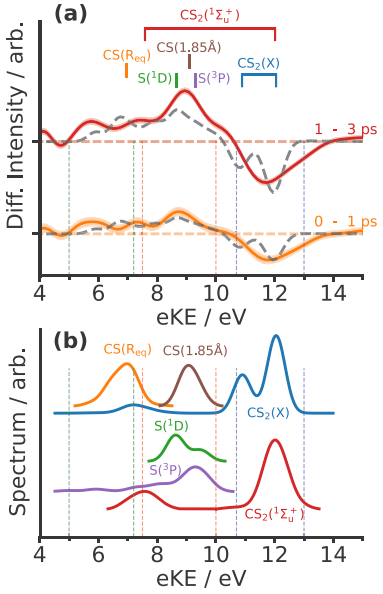

Figure 3. (a) Comparison of experimental and calculated photoelectron difference spectra in two pump−probe delay ranges. Solid lines with shaded error bars show experimental data, while the dashed black lines are obtained from integrating the simulated TRXPS over the same temporal region. The locations of individual calculated fragment spectra are indicated above. (b) Calculated XPS spectra of the CS_2 ground ($\tilde{X}$) and excited ($^1\Sigma_u^+$) states at the Franck−Condon geometry and of the CS and S fragments, scaled by the ionization cross section. "CS(R_{eq})" is computed in the $^1\Sigma_g^+$ ground state at the equilibrium bond geometry with an R_{CS} of 1.54 Å. "CS(1.85 Å)" is computed with an elongated bond length (R_{CS}) of 1.85 Å. The colored vertical dashed lines indicate the corresponding energy integration regions employed in Figure 2. The small features around 7−8 eV in the ground- and excited-state CS_2 spectra are the shakeup peaks that leave the molecule in a valence excited state following core ionization.

https://doi.org/10.1021/acs.jpclett.3c01447
J. Phys. Chem. Lett. 2023, 14, 7126−7133

photoelectron kinetic energy, indicated with the colored dashed lines in panels a and b of Figure 2. The energy-integrated calculated AIMS signals (colored dashed lines in Figure 2c) show rapid enhancements between 6 and 10 eV within the first few hundred femtoseconds before achieving a steady-state signal due to the generation of atomic sulfur and CS photoproducts. While the simulated TRXPS is essential for assigning spectral features to particular atomic and molecular species, the absence of a triplet dissociation channel in the simulated results will result in a different temporal evolution between the measured and calculated spectra. In addition to lacking an ionization signal corresponding to the ^{3}P atomic S product, and assuming that the dissociation is relatively prompt following intersystem crossing, the simulation will exhibit (i) a slower increase in CS product formation and (ii) a longer CS_2 lifetime.

The measured TRXPS, on the contrary, exhibits much slower dynamics than the simulation across all eKE regions, as one can observe in a comparison of the solid and dashed colored traces in Figure 2c. The origin of this discrepancy in time scales is attributed to differences in the preparation of the initial state in the experiment versus the simulation. The excitation pulse is implicitly assumed to be a delta function (i.e., vertical excitation), where the sampled points (taken from a distribution corresponding to the ground vibrational state) are filtered such that the electronic excitation energy falls within the bandwidth of the pump pulse. The resulting vibrational distribution on the $^1\Sigma_u^+$ state in the simulation will be significantly broader than that prepared by the experimental pump pulse, with the latter preparing a specific pair of vibronic states. Figure S1 shows extensive displacements along the asymmetric stretch coordinate, in particular in the initial sampled points. Previous time-resolved studies have established a significant variation in the excited-state lifetime depending on the particular vibrational state that is accessed by the pump process.[22,27,37] In short, the initial conditions for the simulation are more extended in phase space in the excited-state manifold, leading to more prompt dissociation of a significant component of the wave packet.

To ascribe physical meaning to the observed delay-dependent spectral features, we turn to *ab initio* simulations of the photoelectron spectra of the possible photofragments. Figure 3a shows the time-integrated, energy-resolved TRXPS difference signals in various pump−probe delay ranges with features assigned to particular photofragments. Figure 3b shows the fragment spectra computed with a restricted active space configuration interaction (RASCI) method that includes their relative cross sections. The mid-eKE region bounded by the red dashed lines is associated primarily with the stretched diatomic CS fragment, distributed broadly between the equilibrium length and out to a bond length (R_{CS}) of ∼1.85 Å. The stretched CS spectral contributions observed in the data are consistent with the outer turning points of a broad distribution of vibrational states between $v = 0$ and $v = 9$.[38] This is in keeping with the CS fragment vibrational distribution produced by a mixture of singlet and triplet dissociation channels, as measured in previous nanosecond photofragment imaging studies.[23,24] The mid-eKE region also contains contributions from both singlet and triplet atomic sulfur, albeit with smaller ionization cross sections relative to those of the CS photoproduct. The low-eKE region bound by the green dashed lines contains contributions from CS fragments close to their equilibrium bond length. The experimental data in the low-eKE region contain a correspondingly weaker product signal at long time delays than in the mid-eKE region, as one can see from the red curve in Figure 3a.

We performed time-resolved fits to more quantitatively explore the delay dependence of the experimental TRXPS spectral regions assigned to these photoproducts. The fits for the two regions of enhancement (red and green curves in Figure 2c) consisted of an initially populated excited-state contribution that undergoes exponential decay and an exponential rise of signal due to reaction products, as described in eq 1.

$$I(\tau) = A_{exc}\exp(-\tau/\tau_{exc}) + A_{prod}[1 - \exp(-\tau/\tau_{prod})] \quad (1)$$

The region of depletion (blue curve in Figure 2c) was treated in a similar fashion, with a fit consisting of a decaying excited-state signal on top of a negative error function to capture the depletion of the ground-state CS_2 signal blurred by the temporal IRF, as described in eq 2.

$$I(\tau) = A_{exc}\exp(-\tau/\tau_{exc}) - A_{dep}\,\mathrm{erf}(\tau/\tau_{IRF}) \quad (2)$$

The choice to include the excited-state component of the depletion fit was based on both the expectation to observe that signal in the same spectral region as the depletion and a comparison of the reduced χ^2 goodness-of-fit metric χ_ν^2 for fits with and without the excited-state signal. Including the excited state in the fit produced a χ_ν^2 of 1.79, while omitting it produced a χ_ν^2 of 2.76, with values closer to 1 indicating a higher-quality fit. Additional details of the fitting functions and goodness of fit are given in section S6 of the Supporting Information.

The excited-state lifetimes and product rise times in the fits present a complex picture of this reaction in the context of prior measurements. In each case, the least-squares best fit parameter is quoted along with its 1σ uncertainty. The IRF was determined from the fit of the depletion region (blue fit in Figure 2c) to be $\tau_{IRF} = 120 \pm 50$ fs full width at half-maximum (FWHM), in good agreement with the UV pump pulse duration measured during the experiment. The Franck−Condon excited-state $^1\Sigma_u^+$ lifetime (τ_{exc}) of 830 ± 200 fs measured here is in good agreement with the results of Bisgaard et al., who reported an excited-state decay time of 830 fs using time-resolved molecular frame photoelectron angular distributions.[25] Our reported lifetime is also consistent with the lower bounds on the lifetime reported by Townsend et al. (510 ± 30 fs using time-resolved valence photoelectron spectroscopy)[27] and earlier work by Mank and Hepburn (500 ± 100 fs based on the high-resolution S action spectrum line shape).[22] Our measured lifetime is longer but consistent within a 1σ uncertainty to the 630 fs $^1\Sigma_u^+$ lifetime reported by Suzuki and co-workers using time-resolved valence photoelectron spectroscopy.[10] It is important to note that their experiment used a UV pump with a much broader bandwidth that spanned at least four absorption peaks in the CS_2 vibrational progression. It is known that the dissociation lifetime for each of these peaks varies strongly with wavelength,[22] so the time scales measured in these studies cannot be compared directly to those reported here.

The low- and mid-eKE signals in Figure 2c exhibit two distinct photoproduct rise times. The low-eKE region (green curve in Figure 2c), attributed mostly to equilibrium CS, exhibits a rise time (τ_{prod}) of 490 ± 280 fs, consistent with previously quoted excited-state lifetime measurements. This is also roughly consistent with those of Suzuki and co-workers, who reported indistinguishable singlet and triplet sulfur rise times of ∼350 fs.[10] Again, the differences in the pump spectrum between that experiment and ours may account for the minor discrepancies in

https://doi.org/10.1021/acs.jpclett.3c01447
J. Phys. Chem. Lett. 2023, 14, 7126−7133

the time scale. The mid-eKE region (red curve in Figure 2c), attributed at long pump−probe delays to vibrationally hot CS fragments (see Figure 3b) and to atomic sulfur, notably exhibits a much longer photoproduct rise time (τ_{prod}) of 1220 ± 240 fs.

A comparison of the measured time scales of the excited-state decay and rise of photoproducts reveals the inadequacies of a simple kinetic model of this reaction. As the products must proceed in some fashion from the $^1\Sigma_u^+$ state, it is reasonable to expect the rate of excited-state depletion to be equivalent to the effective rate of product formation.

$$\frac{1}{\tau_{exc}} = \sum_i \frac{1}{\tau_{prod}^{(i)}} \tag{3}$$

This is not the case for our measured time constants, as 830^{-1} $fs^{-1} \neq (490^{-1} + 1220^{-1})$ fs^{-1}. The discrepancy suggests that the simplistic kinetic model of the decaying excited-state signal and growth of photoproduct signal used here is insufficient to describe the data accurately. Improved models could incorporate time-dependent coupling rates from the excited state into the various photoproduct channels, such as the one suggested for this reaction by Minns and co-workers that included a suppression of the singlet dissociation channel after a few hundred femtoseconds.[7] We furthermore note that the use of a kinetic model fails to fully capture the underlying quantum dynamics in prior work as well (such as the revival of the initial coherence at an ∼1 ps time delay observed by Suzuki and co-workers[10]). We believe that, ultimately, these types of ultrafast photodissociation problems can be better understood in terms of a coherent superposition of compound scattering resonances that interfere as they decay, as was previously described in the non-adiabatic photodissociation of IBr.[39] Nevertheless, kinetic models are still useful as a means of intuitively quantifying time-dependent results as opposed to a faithful model of the process.

In conclusion, we have presented a combined experimental and theoretical TRXPS study of the UV-induced multichannel photodissociation of CS_2. We find that both the photoexcitation and the subsequent large-amplitude motion produce rapid S 2p spectral shifts. Comparison of experimental data with state-of-the-art *ab initio* simulations shows that the S 2p spectrum depends strongly on whether the probed sulfur atom is a bare atom or a member of a CS fragment or CS_2 molecule as well as whether the diatomic fragment is in its vibrational ground or excited states. Quantification of reaction time scales using TRXPS and comparison to prior valence studies reveal the complex nature of this reaction and the inadequacies of some kinetic models commonly employed to describe it. These results demonstrate the sensitivity of the TRXPS technique to multimodal molecular motion in the gas phase more generally, crucially including both signatures of the transient bound excited state and the vibrational states of the photoproducts in addition to providing a multifaceted picture of the reaction kinetics. In the case of CS_2, the spectral overlap and varying ionization cross sections of different fragments present some challenges for TRXPS in separating their individual contributions. This motivates the use of channel-resolved analysis techniques such as electron−ion covariance to correlate weaker photoelectron spectral signatures to particular ionic fragments in a background-free manner.[12,19,40] TRXPS will also benefit greatly from the ongoing developments in seeded and high-repetition rate FELs,[41] allowing large volumes of data to be recorded at high energy resolution in a short acquisition period. This will further increase the applicability of TRXPS, for instance, by enabling one to scan the probe photon energy and thus probe various core sites within a molecule during a single experiment.

METHODS

Experiments were performed at the FLASH free-electron laser[31] at beamline BL1 at the CAMP instrument using an experimental setup broadly similar to one outlined previously.[32,42] CS_2 was introduced into the spectrometer as a skimmed supersonic molecular beam. An ultraviolet femtosecond pump pulse (λ = 201.5 nm, 200 nJ, 120 fs FWHM, 10 Hz repetition rate) was used to photoexcite the sample, and the ensuing dynamics were probed by using photoionization at the S 2p edge using a soft X-ray FEL pulse ($\hbar\omega$ = 181.5 eV, 50 μJ, 90 fs FWHM). Photoelectrons and photoions (not shown) produced from inner-shell ionization were detected as a function of pump−probe delay and kinetic energy using the double-sided VMI spectrometer. Temporal overlap ("time zero") was determined through prompt enhancements in the ion momentum distributions for various fragments, and corrections to the jitter of the X-ray and laser arrival time were performed using a procedure outlined in prior work.[43,44] The presented photoelectron spectrum was constructed via Abel-inverting the summed electron VMI image at each pump−probe delay, and the difference signal was calculated by subtracting the average negative delay photoelectron spectrum from the time-resolved signal. Further details of the experimental apparatus are provided in the Supporting Information.

The dynamics simulations were performed using the AIMS method[34] in which the coupled potential energy surfaces and non-adiabatic couplings were determined on the fly at the ANO(4s3p2d/3s2p1d)/MR-CIS(10,8) level of theory. The X-ray photoelectron spectra were determined by employing spin−orbit RASCI computations for both the valence excited and core-ionized states. The ionization cross sections were approximated using the corresponding Dyson orbital norms between the neutral and cationic states. Further details for technical elements of the simulations are provided in the Supporting Information.

ASSOCIATED CONTENT

Supporting Information

The Supporting Information is available free of charge at https://pubs.acs.org/doi/10.1021/acs.jpclett.3c01447.

AIMS trajectory details (section S1), simulation of fragment spectra (section S2), simulation of time-resolved spectra (section S3), experimental details (section S4), data processing (section S5), fitting analysis of the TRXPS signal (section S6), and author contributions (section S7) (PDF)

Transparent Peer Review report available (PDF)

AUTHOR INFORMATION

Corresponding Authors

Michael S. Schuurman − *National Research Council Canada, Ottawa, Ontario K1A 0R6, Canada; Department of Chemistry and Biomolecular Sciences, University of Ottawa, Ottawa, Ontario K1N 6N5, Canada;* orcid.org/0000-0002-0922-9034; Email: michael.schuurman@uottawa.ca

Ruaridh Forbes − *Linac Coherent Light Source, SLAC National Accelerator Laboratory, Menlo Park, California*

https://doi.org/10.1021/acs.jpclett.3c01447
J. Phys. Chem. Lett. 2023, 14, 7126−7133

94025, United States; orcid.org/0000-0003-2097-5991; Email: ruforbes@slac.stanford.edu

Authors

Ian Gabalski − *Stanford PULSE Institute, SLAC National Accelerator Laboratory, Menlo Park, California 94025, United States; Department of Applied Physics, Stanford University, Stanford, California 94305, United States;* orcid.org/0000-0002-6782-6566

Felix Allum − *Stanford PULSE Institute, SLAC National Accelerator Laboratory, Menlo Park, California 94025, United States; Linac Coherent Light Source, SLAC National Accelerator Laboratory, Menlo Park, California 94025, United States; Chemistry Research Laboratory, Department of Chemistry, University of Oxford, Oxford OX1 3TA, U.K.;* orcid.org/0000-0002-8044-8969

Issaka Seidu − *National Research Council Canada, Ottawa, Ontario K1A 0R6, Canada*

Mathew Britton − *Stanford PULSE Institute, SLAC National Accelerator Laboratory, Menlo Park, California 94025, United States*

Günter Brenner − *Deutsches Elektronen-Synchrotron DESY, 22607 Hamburg, Germany*

Hubertus Bromberger − *Deutsches Elektronen-Synchrotron DESY, 22607 Hamburg, Germany*

Mark Brouard − *Chemistry Research Laboratory, Department of Chemistry, University of Oxford, Oxford OX1 3TA, U.K.;* orcid.org/0000-0003-3421-0850

Philip H. Bucksbaum − *Stanford PULSE Institute, SLAC National Accelerator Laboratory, Menlo Park, California 94025, United States; Department of Applied Physics, Stanford University, Stanford, California 94305, United States; Department of Physics, Stanford University, Stanford, California 94305, United States*

Michael Burt − *Chemistry Research Laboratory, Department of Chemistry, University of Oxford, Oxford OX1 3TA, U.K.;* orcid.org/0000-0002-7317-8649

James P. Cryan − *Stanford PULSE Institute, SLAC National Accelerator Laboratory, Menlo Park, California 94025, United States; Linac Coherent Light Source, SLAC National Accelerator Laboratory, Menlo Park, California 94025, United States;* orcid.org/0000-0002-7776-0919

Taran Driver − *Stanford PULSE Institute, SLAC National Accelerator Laboratory, Menlo Park, California 94025, United States; Linac Coherent Light Source, SLAC National Accelerator Laboratory, Menlo Park, California 94025, United States;* orcid.org/0000-0002-3761-6883

Nagitha Ekanayake − *Deutsches Elektronen-Synchrotron DESY, 22607 Hamburg, Germany*

Benjamin Erk − *Deutsches Elektronen-Synchrotron DESY, 22607 Hamburg, Germany;* orcid.org/0000-0001-8413-3588

Diksha Garg − *Deutsches Elektronen-Synchrotron DESY, 22607 Hamburg, Germany*

Eva Gougoula − *Deutsches Elektronen-Synchrotron DESY, 22607 Hamburg, Germany*

David Heathcote − *Chemistry Research Laboratory, Department of Chemistry, University of Oxford, Oxford OX1 3TA, U.K.*

Paul Hockett − *National Research Council Canada, Ottawa, Ontario K1A 0R6, Canada*

David M. P. Holland − *Daresbury Laboratory, Warrington, Cheshire WA4 4AD, U.K.*

Andrew J. Howard − *Stanford PULSE Institute, SLAC National Accelerator Laboratory, Menlo Park, California 94025, United States; Department of Applied Physics, Stanford University, Stanford, California 94305, United States*

Sonu Kumar − *Deutsches Elektronen-Synchrotron DESY, 22607 Hamburg, Germany*

Jason W. L. Lee − *Deutsches Elektronen-Synchrotron DESY, 22607 Hamburg, Germany*

Siqi Li − *Linac Coherent Light Source, SLAC National Accelerator Laboratory, Menlo Park, California 94025, United States*

Joseph McManus − *Chemistry Research Laboratory, Department of Chemistry, University of Oxford, Oxford OX1 3TA, U.K.;* orcid.org/0000-0002-7911-2042

Jochen Mikosch − *Institut für Physik, Universität Kassel, 34132 Kassel, Germany*

Dennis Milesevic − *Chemistry Research Laboratory, Department of Chemistry, University of Oxford, Oxford OX1 3TA, U.K.*

Russell S. Minns − *School of Chemistry, University of Southampton, Southampton SO17 1BJ, U.K.*

Simon Neville − *National Research Council Canada, Ottawa, Ontario K1A 0R6, Canada;* orcid.org/0000-0001-8134-1883

Atia-Tul-Noor − *Deutsches Elektronen-Synchrotron DESY, 22607 Hamburg, Germany*

Christina C. Papadopoulou − *Deutsches Elektronen-Synchrotron DESY, 22607 Hamburg, Germany*

Christopher Passow − *Deutsches Elektronen-Synchrotron DESY, 22607 Hamburg, Germany*

Weronika O. Razmus − *School of Chemistry, University of Southampton, Southampton SO17 1BJ, U.K.*

Anja Röder − *Max-Born-Institute, 12489 Berlin, Germany*

Arnaud Rouzée − *Max-Born-Institute, 12489 Berlin, Germany*

Alcides Simao − *Deutsches Elektronen-Synchrotron DESY, 22607 Hamburg, Germany*

James Unwin − *Chemistry Research Laboratory, Department of Chemistry, University of Oxford, Oxford OX1 3TA, U.K.*

Claire Vallance − *Chemistry Research Laboratory, Department of Chemistry, University of Oxford, Oxford OX1 3TA, U.K.;* orcid.org/0000-0003-3880-8614

Tiffany Walmsley − *Chemistry Research Laboratory, Department of Chemistry, University of Oxford, Oxford OX1 3TA, U.K.*

Jun Wang − *Stanford PULSE Institute, SLAC National Accelerator Laboratory, Menlo Park, California 94025, United States; Department of Applied Physics, Stanford University, Stanford, California 94305, United States;* orcid.org/0000-0003-1962-895X

Daniel Rolles − *J. R. Macdonald Laboratory, Department of Physics, Kansas State University, Manhattan, Kansas 66506, United States;* orcid.org/0000-0002-3965-3477

Albert Stolow − *National Research Council Canada, Ottawa, Ontario K1A 0R6, Canada; Department of Physics and Department of Chemistry and Biomolecular Sciences, University of Ottawa, Ottawa, Ontario K1N 6N5, Canada; NRC-uOttawa Joint Centre for Extreme Photonics, Ottawa, Ontario K1A 0R6, Canada;* orcid.org/0000-0002-8447-3678

Complete contact information is available at: https://pubs.acs.org/10.1021/acs.jpclett.3c01447

https://doi.org/10.1021/acs.jpclett.3c01447
J. Phys. Chem. Lett. 2023, 14, 7126−7133

Notes

The authors declare no competing financial interest.

■ ACKNOWLEDGMENTS

The authors acknowledge DESY (Hamburg, Germany), a member of the Helmholtz Association HGF, for the provision of experimental facilities. Parts of this research were carried out at FLASH. Beamtime was allocated for Proposal F-20200773. The research was further supported by the CALIPSOplus project under Grant Agreement 730872 from the EU Framework Programme for Research and Innovation HORIZON 2020. This research was supported in part through the Maxwell computational resources operated at Deutsches Elektronen-Synchrotron DESY (Hamburg, Germany). The authors gratefully acknowledge the work of the scientific and technical teams at FLASH. The authors acknowledge the Max Planck Society for funding the development and the initial operation of the CAMP end-station within the Max Planck Advanced Study Group at CFEL and for providing this equipment for CAMP@FLASH. The installation of CAMP@FLASH was partially funded by BMBF Grants 05K10KT2, 05K13KT2, 05K16KT3, and 05K10KTB from FSP-302. R.F. and F.A. gratefully acknowledge support from the Linac Coherent Light Source, SLAC National Accelerator Laboratory, which is supported by the U.S. Department of Energy, Office of Science, Office of Basic Energy Sciences, under Contract DE-AC02-76SF00515. J.P.C. and P.H.B. are supported by the U.S. Department of Energy, Office of Science, Basic Energy Sciences (BES), Chemical Sciences, Geosciences, and Biosciences Division, AMOS Program. D.R. is supported by National Science Foundation (NSF) Grant PHYS-1753324 and is thankful to LCLS and the Stanford PULSE Institute for their hospitality and financial support during a sabbatical. I.G. was supported by a NDSEG Fellowship. A. Stolow thanks the NRC-uOttawa Joint Centre for Extreme Photonics (JCEP) for financial support. A. Stolow and M.S.S. thank the NSERC Discovery Grants program and NRC CSTIP Quantum Sensors Project QSP-075-1 for financial support. J.U., T.W., and M. Burt are grateful for support from the UK EPSRC (EP/S028617/1). A CC-BY license is applied to the author-accepted manuscript arising from this submission, in accordance with UKRI open access conditions. J.U. is also grateful to the States of Jersey for studentship funding. T.W. additionally thanks the UK EPSRC and Jesus College, Oxford, for studentship funding. J.W.L.L. acknowledges financial support from the Helmholtz-ERC Recognition Award (ERC-RA-0043) of the Helmholtz Association (HGF). W.O.R. thanks the University of Southampton and the STFC XFEL hub for physical sciences for a Ph.D. studentship. R.S.M. gratefully acknowledges financial support from the EPSRC (EP/R010609/1) and the Leverhulme Trust (RPG-2021-257). C.V., D.H., and M. Brouard acknowledge support from EPSRC Programme Grants EP/V026690/1 and EP/T021675/1. D.M.P.H. is grateful to the Science and Technology Facilities Council (United Kingdom) for financial support. J. Mikosch gratefully acknowledges funding from the European Research Council (ERC) under the European Union's Horizon 2020 research and innovation programme within a Consolidator Grant (CoG Agreement 101003142).

■ REFERENCES

(1) Stolow, A.; Bragg, A. E.; Neumark, D. M. Femtosecond Time-Resolved Photoelectron Spectroscopy. *Chem. Rev.* **2004**, *104*, 1719−1758.

(2) Suzuki, T. Femtosecond Time-resolved Photoelectron Imaging. *Annu. Rev. Phys. Chem.* **2006**, *57*, 555−592.

(3) Neumark, D. M. Time-Resolved Photoelectron Spectroscopy of Molecules and Clusters. *Annu. Rev. Phys. Chem.* **2001**, *52*, 255−277.

(4) Schuurman, M. S.; Blanchet, V. Time-Resolved Photoelectron Spectroscopy: The Continuing Evolution of a Mature Technique. *Phys. Chem. Chem. Phys.* **2022**, *24*, 20012−20024.

(5) Schuurman, M. S.; Stolow, A. Dynamics at Conical Intersections. *Annu. Rev. Phys. Chem.* **2018**, *69*, 427−450.

(6) Stolow, A.; Underwood, J. G. *Advances in Chemical Physics*; Wiley: Hoboken, NJ, 2008; Vol. *139*.

(7) Smith, A. D.; Warne, E. M.; Bellshaw, D.; Horke, D. A.; Tudorovskya, M.; Springate, E.; Jones, A. J. H.; Cacho, C.; Chapman, R. T.; Kirrander, A.; Minns, R. S. Mapping the Complete Reaction Path of a Complex Photochemical Reaction. *Phys. Rev. Lett.* **2018**, *120*, 183003.

(8) Spesyvtsev, R.; Horio, T.; Suzuki, Y.-I.; Suzuki, T. Observation of the Wavepacket Dynamics on the $^1B_2(^1\Sigma_u^+)$ State of CS_2 by Sub-20 fs Photoelectron Imaging Using 159 nm Probe Pulses. *J. Chem. Phys.* **2015**, *142*, 074308.

(9) Horio, T.; Spesyvtsev, R.; Furumido, Y.; Suzuki, T. Real-Time Detection of $S(^1D_2)$ Photofragments Produced from the $^1B_2(^1\Sigma_u^+)$ State of CS_2 by Vacuum Ultraviolet Photoelectron Imaging Using 133 nm Probe Pulses. *J. Chem. Phys.* **2017**, *147*, 013932.

(10) Karashima, S.; Suzuki, Y.-I.; Suzuki, T. Ultrafast Extreme Ultraviolet Photoelectron Spectroscopy of Nonadiabatic Photodissociation of CS_2 from $^1B_2(^1\Sigma_u^+)$ State: Product Formation via an Intermediate Electronic State. *J. Phys. Chem. Lett.* **2021**, *12*, 3755−3761.

(11) Warne, E. M.; Smith, A. D.; Horke, D. A.; Springate, E.; Jones, A. J. H.; Cacho, C.; Chapman, R. T.; Minns, R. S. Time Resolved Detection of the $S(^1D)$ Product of the UV Induced Dissociation of CS_2. *J. Chem. Phys.* **2021**, *154*, 034302.

(12) Boguslavskiy, A. E.; Schalk, O.; Gador, N.; Glover, W. J.; Mori, T.; Schultz, T.; Schuurman, M. S.; Martínez, T. J.; Stolow, A. Excited State Non-Adiabatic Dynamics of the Smallest Polyene, Trans 1,3-Butadiene. I. Time-resolved Photoelectron-Photoion Coincidence Spectroscopy. *J. Chem. Phys.* **2018**, *148*, 164302.

(13) Coates, M. R.; Larsen, M. A. B.; Forbes, R.; Neville, S. P.; Boguslavskiy, A. E.; Wilkinson, I.; Sølling, T. I.; Lausten, R.; Stolow, A.; Schuurman, M. S. Vacuum Ultraviolet Excited State Dynamics of the Smallest Ring, Cyclopropane. II. Time-resolved Photoelectron Spectroscopy and Ab Initio Dynamics. *J. Chem. Phys.* **2018**, *149*, 144311.

(14) Forbes, R.; Neville, S. P.; Larsen, M. A. B.; Röder, A.; Boguslavskiy, A. E.; Lausten, R.; Schuurman, M. S.; Stolow, A. Vacuum Ultraviolet Excited State Dynamics of the Smallest Ketone: Acetone. *J. Phys. Chem. Lett.* **2021**, *12*, 8541−8547.

(15) Williams, M.; Forbes, R.; Weir, H.; Veyrinas, K.; MacDonell, R. J.; Boguslavskiy, A. E.; Schuurman, M. S.; Stolow, A.; Martinez, T. J. Unmasking the Cis-Stilbene Phantom State via Vacuum Ultraviolet Time-Resolved Photoelectron Spectroscopy and Ab Initio Multiple Spawning. *J. Phys. Chem. Lett.* **2021**, *12*, 6363−6369.

(16) Glover, W. J.; Mori, T.; Schuurman, M. S.; Boguslavskiy, A. E.; Schalk, O.; Stolow, A.; Martínez, T. J. Excited State Non-Adiabatic Dynamics of the Smallest Polyene, Trans 1,3-Butadiene. II. Ab Initio Multiple Spawning Simulations. *J. Chem. Phys.* **2018**, *148*, 164303.

(17) Leitner, T.; Josefsson, I.; Mazza, T.; Miedema, P. S.; Schröder, H.; Beye, M.; Kunnus, K.; Schreck, S.; Düsterer, S.; Föhlisch, A.; Meyer, M.; Odelius, M.; Wernet, Ph. Time-Resolved Electron Spectroscopy for Chemical Analysis of Photodissociation: Photoelectron Spectra of $Fe(CO)_5$, $Fe(CO)_4$, and $Fe(CO)_3$. *J. Chem. Phys.* **2018**, *149*, 044307.

(18) Brausse, F.; et al. Time-Resolved Inner-Shell Photoelectron Spectroscopy: From a Bound Molecule to an Isolated Atom. *Phys. Rev. A* **2018**, *97*, 043429.

(19) Allum, F.; et al. A Localized View on Molecular Dissociation via Electron-Ion Partial Covariance. *Commun. Chem.* **2022**, *5*, 42.

(20) Mayer, D.; et al. Following Excited-State Chemical Shifts in Molecular Ultrafast X-ray Photoelectron Spectroscopy. *Nat. Commun.* **2022**, *13*, 198.

https://doi.org/10.1021/acs.jpclett.3c01447
J. Phys. Chem. Lett. 2023, 14, 7126−7133

(21) Santra, R.; Kryzhevoi, N. V.; Cederbaum, L. S. X-Ray Two-Photon Photoelectron Spectroscopy: A Theoretical Study of Inner-Shell Spectra of the Organic Para-Aminophenol Molecule. *Phys. Rev. Lett.* **2009**, *103*, 013002.
(22) Mank, A.; Starrs, C.; Jego, M. N.; Hepburn, J. W. A Detailed Study of the Predissociation Dynamics of the $^1B_2(^1\Sigma_u^+)$ State of CS_2. *J. Chem. Phys.* **1996**, *104*, 3609−3619.
(23) Campbell, E. K. Atomic Polarisation in Molecular Photodissociation. Ph.D. Thesis, University of Oxford, Oxford, U.K., 2016.
(24) Zhao, M.; Li, Z.-x.; Xie, T.; Chang, Y.; Wu, F.-y.; Wang, Q.; Chen, W.-t.; Wang, T.; Wang, X.-a.; Yuan, K.-j.; Yang, X.-m. Photodissociation Dynamics of CS_2 near 204 nm: The $S(^3P_J)$+$CS(X^1\Sigma^+)$ Channels. *Chin. J. Chem. Phys.* **2021**, *34*, 95−101.
(25) Bisgaard, C. Z.; Clarkin, O. J.; Wu, G.; Lee, A. M. D.; Geßner, O.; Hayden, C. C.; Stolow, A. Time-Resolved Molecular Frame Dynamics of Fixed-in-Space CS_2 Molecules. *Science* **2009**, *323*, 1464−1468.
(26) Hockett, P.; Bisgaard, C. Z.; Clarkin, O. J.; Stolow, A. Time-Resolved Imaging of Purely Valence-Electron Dynamics during a Chemical Reaction. *Nat. Phys.* **2011**, *7*, 612−615.
(27) Townsend, D.; Satzger, H.; Ejdrup, T.; Lee, A. M. D.; Stapelfeldt, H.; Stolow, A. $^1B_2(^1\Sigma_u^+)$ Excited State Decay Dynamics in CS_2. *J. Chem. Phys.* **2006**, *125*, 234302.
(28) Razmus, W. O.; et al. Multichannel Photodissociation Dynamics in CS_2 Studied by Ultrafast Electron Diffraction. *Phys. Chem. Chem. Phys.* **2022**, *24*, 15416.
(29) Gabalski, I.; et al. Transient Vibration and Product Formation of Photoexcited CS_2 Measured by Time-Resolved X-ray Scattering. *J. Chem. Phys.* **2022**, *157*, 164305.
(30) Coville, M.; Thomas, T. D. Sulfur 2p Ionization Energies of H_2S, OCS, SO_2, and CS_2. *J. Electron Spectrosc. Relat.* **1995**, *71*, 21−23.
(31) Ackermann, W.; et al. Operation of a Free-Electron Laser from the Extreme Ultraviolet to the Water Window. *Nat. Photonics* **2007**, *1*, 336−342.
(32) Erk, B.; et al. CAMP@FLASH: An End-Station for Imaging, Electron- and Ion-Spectroscopy, and Pump−Probe Experiments at the FLASH Free-Electron Laser. *J. Synchrotron Radiat.* **2018**, *25*, 1529−1540.
(33) Unwin, J. X-ray Induced Coulomb Explosion Imaging of Transient Excited-State Structural Rearrangements in CS_2. **2023** (under review).
(34) Ben-Nun, M.; Quenneville, J.; Martínez, T. J. Ab Initio Multiple Spawning: Photochemistry from First Principles Quantum Molecular Dynamics. *J. Phys. Chem. A* **2000**, *104*, 5161−5175.
(35) Li, S.; Driver, T.; Alexander, O.; Cooper, B.; Garratt, D.; Marinelli, A.; Cryan, J. P.; Marangos, J. Time-Resolved Pump−Probe Spectroscopy with Spectral Domain Ghost Imaging. *Faraday Discuss.* **2021**, *228*, 488−501.
(36) Wang, J.; Driver, T.; Allum, F.; Papadopoulou, C. C.; Passow, C.; Brenner, G.; Li, S.; Düsterer, S.; Noor, A. T.; Kumar, S.; Bucksbaum, P. H.; Erk, B.; Forbes, R.; Cryan, J. P. Photon Energy-Resolved Velocity Map Imaging from Spectral Domain Ghost Imaging. *New J. Phys.* **2023**, *25*, 033017.
(37) Farmanara, P.; Stert, V.; Radloff, W. Ultrafast Predissociation and Coherent Phenomena in CS_2 Excited by Femtosecond Laser Pulses at 194−207 nm. *J. Chem. Phys.* **1999**, *111*, 5338−5343.
(38) Nair, K. P. R.; Singh, R. B.; Rai, D. K. Potential-Energy Curves and Dissociation Energies of Oxides and Sulfides of Group IV A Elements. *J. Chem. Phys.* **1965**, *43*, 3570−3574.
(39) Shapiro, M.; Vrakking, M. J. J.; Stolow, A. Nonadiabatic Wave Packet Dynamics: Experiment and Theory in IBr. *J. Chem. Phys.* **1999**, *110*, 2465−2473.
(40) Boguslavskiy, A. E.; Mikosch, J.; Gijsbertsen, A.; Spanner, M.; Patchkovskii, S.; Gador, N.; Vrakking, M. J. J.; Stolow, A. The Multielectron Ionization Dynamics Underlying Attosecond Strong-Field Spectroscopies. *Science* **2012**, *335*, 1336−1340.
(41) Beye, M.; Gühr, M.; Hartl, I.; Plönjes, E.; Schaper, L.; Schreiber, S.; Tiedtke, K.; Treusch, R. FLASH and the FLASH2020+ Project—Current Status and Upgrades for the Free-Electron Laser in Hamburg at DESY. *Eur. Phys. J. Plus* **2023**, *138*, 193.
(42) Forbes, R.; Allum, F.; Bari, S.; Boll, R.; Borne, K.; Brouard, M.; Bucksbaum, P. H.; Ekanayake, N.; Erk, B.; Howard, A. J.; et al. Time-Resolved Site-Selective Imaging of Predissociation and Charge Transfer Dynamics: The CH_3I B-band. *J. Phys. B: At., Mol. Opt. Phys.* **2020**, *53*, 224001.
(43) Löhl, F.; Arsov, V.; Felber, M.; Hacker, K.; Jalmuzna, W.; Lorbeer, B.; Ludwig, F.; Matthiesen, K.-H.; Schlarb, H.; Schmidt, B.; Schmüser, P.; Schulz, S.; Szewinski, J.; Winter, A.; Zemella, J. Electron Bunch Timing with Femtosecond Precision in a Superconducting Free-Electron Laser. *Phys. Rev. Lett.* **2010**, *104*, 144801.
(44) Savelyev, E.; Boll, R.; Bomme, C.; Schirmel, N.; Redlin, H.; Erk, B.; Düsterer, S.; Müller, E.; Höppner, H.; Toleikis, S.; et al. Jitter-Correction for IR/UV-XUV Pump-Probe Experiments at the FLASH Free-Electron Laser. *New J. Phys.* **2017**, *19*, 043009.

https://doi.org/10.1021/acs.jpclett.3c01447
J. Phys. Chem. Lett. 2023, 14, 7126−7133